CHEMICAL ENGINEERING TRANSACTIONS

VOL. 55, 2016

A publication of AIDIC
The Italian Association of Chemical Engineering
Online at www.aidic.it/cet

Guest Editors: Tichun Wang, Hongyang Zhang, Lei Tian

ISBN 978-88-95608-46-4; **ISSN** 2283-9216

DOI: 10.3303/CET1655006

Vibration Response of an Existing Tunnel to Adjacent Blasting Construction

Yuan Zhou*[a,b], She L. Wang[b], Juan Wang[a]
[a] College of Science, Chang'an University, China;
[b] School of Civil Engineering, Xi`an University of Architecture and Technology, China.
1426673867@qq.com

With tunnels as the engineering background, we established a mathematic model between an existing tunnel and the adjacent tunnel under construction at different values of spacing. Analysis was conducted on the vibration response of the existing tunnel to adjacent blasting construction. Accordingly, we obtained the vibration velocity point layout scheme and the corresponding explosive loading optimization scheme: measurement points for the existing tunnel should be distributed over the middle-top front straight wall. The measurement point of fastest vibration is 4m before the tunnel face counterpart. Key monitoring should be done on the interval of -4m~10m from the tunnel face. By comparing the numerical simulation result with the measured data, we conclude that the measured peak vibration velocity and the numerical results basically share the same change trend. Proper control over explosive loading is crucial to diminishing blasting-induced vibration response and realizing normal operation of existing tunnels.

1. Introduction

Along with huge leaps in national economy and transportation engineering in China, an increasing number of double-line construction projects has been initiated and are under way. Restricted by topography and geology, the design spacing between newly-built tunnels and existing tunnels is limited to a certain value for most of the cases. For example, the middle wall that separates the Baocheng double-track railroad and the existing tunnel is 1.902~2.323m thick; the minimum spacing between the New Dacheng Tunnel of the Second Xiangyu Railway and the existing railroad line is merely 3.73m (Wang et al., 2010), for Zhaobao Mountain Tunnel, known as a new double-track highway tunnel, the design spacing between the tracks is as small as 2.98-4.20m (Liu, 2010). The net width of the rock pillar of Xianyue Mountain Tunnel, a small-spacing double-hole four-lane tunnel in Xiamen city, is 19m (Li, 2010). The spacing between the Qingshan tunnels of Neijiang-Kunming Line only ranges from 2.76m to 12.8m. The recently completed second track of Xi'an-Ankang Railway is 8m far from the existing Xiaoyu Tunnel with respect to the minimum vertical spacing. During the process of railway tunnel construction, the drill and blast method receives widespread application due to flexible adaptiveness, low cost and fast construction. Blasting-induced seismic waves will transmit through rock mediums and subsequently vibrate particles along the path (Zhao and Wang, 2007). Such oscillation, if strong enough, will do harm to engineering by destroying the surrounding rock and/or existing constructions and the like. Therefore, blasting-induced vibration poses threats to the safety of neighboring tunnels and incurs stress redistribution for surrounding rocks of existing tunnels, especially for rocks of medium-to-high hardness (Tan et al., 2003).
In small spacing conditions, the blasting vibration effect generated during construction of new tunnels may endanger the structure and normal operation of existing tunnels to a large extent. Given this, the drilling and blast construction work for small-spacing tunnels should be conducted under the guidance of sound and effective detonation schemes. This is aimed at rendering the destructive power of blasting vibration controllable as well as guaranteeing both the safety of current normal operation and the quality and progress of ongoing tunnel construction. What is more, efforts should be stepped up to monitor, measure and analyze parameters of existing tunnels in real time, so that ensuring the security of tunnel structure and its operation status.

Please cite this article as: Zhou Y., Wang S.L., Wang J., 2016, Vibration response of an existing tunnel to adjacent blasting construction, Chemical Engineering Transactions, 55, 31-36 DOI:10.3303/CET1655006

A double-tunnel 3D model was established in this paper with the LS-DYNA dynamic finite element software. We also proposed a pair of schemes concerning vibration velocity measurement layout for existing tunnels and the corresponding explosive loading for the neighboring tunnel under construction. Through a comparative analysis of numerical test results and actual measurements, we obtained the following findings: as the tunnel spacing continues decreasing, the change trend of actual peak particle velocities is analogous to that of corresponding numerical results; the key to the structural safety of existing tunnels ensured by reducing its response to blasting vibration is to control explosive loading in a reasonable and efficacious manner. These research conclusions can serve for blasting tunnel construction in small spacing conditions, because it offsets the poor predictability and hysteresis of some popular blasting strength monitoring methods in engineering practice. By applying these findings to engineering practice, the perniciousness of blasting-induced vibration can be controlled actively towards the normal operation of existing tunnels.

2. Engineering introduction

Xi'an-Ankang Railway passes across southern Shaanxi province, with Longhai railway, Baoxi railway, Xiping railway and Zhengzhou-Xi'an Motor Transport to its north and Xiangyu Railway and Yang'an railway to its south. It is located at the junction of middle and western parts of China, and traverses Qinling Mountains—the geological north-south watershed. It serves the major connection between areas in northern, middle and partially eastern China and areas in southwestern China, known as the vital component of Baoliu railway, one of the arteries of eight vertical and eight horizontal high-speed rail networks across the country.

Our research targets at one small-spacing tunnel No.2 within the XKS-1 section of the Second Xi'an-Ankang Railway (as shown in Figure 1a), which lies in the northern piedmont of middle-low Qinling mountains. In terms of tunnel No.2 parameters, the deepest depth is about 210m; the depth of small-spacing section falls into the range of 130-150m; the tunnel is 398m long; the beginning and end mileage: DK79+993~K80+391, where the spacing between the newly-built tunnel and the existing Dapiaogou tunnel at DK80+354~DK80+391 section is 4.8~10m, and 10~19m at DK80+326~DK80+354 section. The hard and well-integrated surrounding rocks of the new tunnel are mainly Class II-III. The underground water is largely oligotrophic or weakly eutrophic. The design cross section of tunnel is U-shape, whose size is shown in Figure 1b. This tunnel is the control engineering work of the Second Xi'an-Ankang Railway.

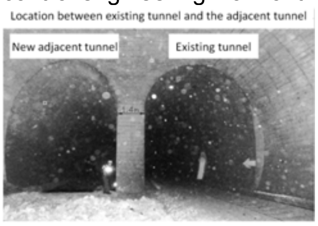

Figure 1(a): small-spacing tunnel

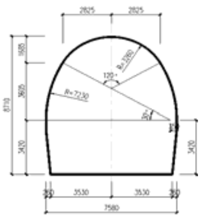

Figure 1(b): Cross-section of the new building tunnel

3. Numerical computation model and result analysis

3.1 Numerical computation model

The model diameter of the cartridge bag is 32mm, the same as the actual one. According to document (Zhong et al., 2010) the boundary effect is negligible if the length of the model boundary is over 3 times the excavation diameter. Therefore, we let the front-rear boundary be 40m, the distances of upper and lower boundaries from tunnel top and bottom be 10m and 15m, respectively, and the left and right boundaries be 15m far from tunnel face. The corresponding finite element model is shown in Figure 2a. The plane map of tunnel locations is displayed in Figure 2b. The axes X, Y and Z of the 3D model are separately along the vertical direction, the plumping direction and the excavation direction. A three-dimensional constraint is forced on the model bottom, and the rest remains as free surfaces. To diminish the boundary effect, we let the left, right, upper and lower model boundaries be non-reflecting boundaries.

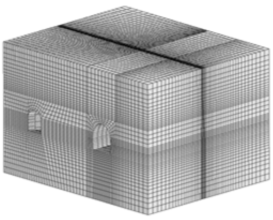

Figure 2(a): Tunnelmodel

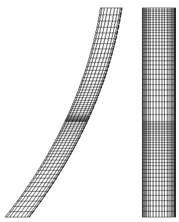

Figure 2(b): Plane relation of the two tunnels

During engineering calculation, the initial stress field must be given priority. In order to reflect the actual working conditions, our simulation was conducted under the action of the initial ground stress. As the actual depth of small-spacing section falls into the range of 140-160m, we exerted an initial ground stress on the model at the tunnel depth of 150m, i.e. the upper boundary was under the action of vertical stresses pursuant to gravity loads. The lateral pressure coefficient of 0.6. The SOLID185 unit and the SHELL181 unit are separately used to find the solutions for parameters of surrounding rocks, explosives and air as well as lining, both of which can produce explicit-implicit constant solutions. The multi-material ALE algorithm was used to calculate the shared nodes of explosives, air and surrounding rocks by using m-kg-s SI units.

3.2 Determination of the location of in-situ vibration monitoring points for the existing tunnel

MAT_PLASTIC_KINEMATIC was used to simulate rock, MAT_NULL was employed to model air, with the use of the linear polynomial EOS, where the initial density was set as 1.293×10-3 Kg/cm3 and the initial energy density as 0.2533MPa. The rock emulsion explosives that are frequently used in engineering practice were used here, whose unit material simulation model was MAT_HIGH_EXPLOSIVE_BURN.

During our searching for a reasonable layout of in-situ vibration monitoring points for the existing tunnel, we took the DK80+354 blasting cross section as an example for computation and simulation.

(1) The law of radial vibration velocity distribution

There are all together 12 measurement points along the radial direction, whose positions are shown in Figure 3. These points have basically covered all key tunnel parts, with three of them are at the front straight wall, three at the rear straight wall, three at the bottom plate, one at the left arch haunch, one at the right arch haunch, and one at the arch crown. On the right side of the figure is the front. Figure 4 is the three-direction vibration time history curves of the dozen of points. We plotted the envelop map of radial velocity (cm/s) in Figure 5, in an attempt to expound the law of radial vibration velocity change deeply.

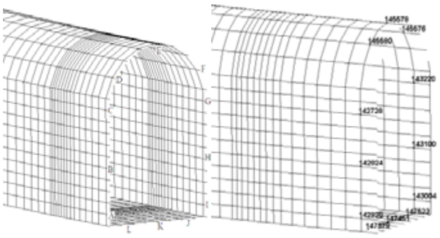

Figure 3: layout of 12 radial measurement points

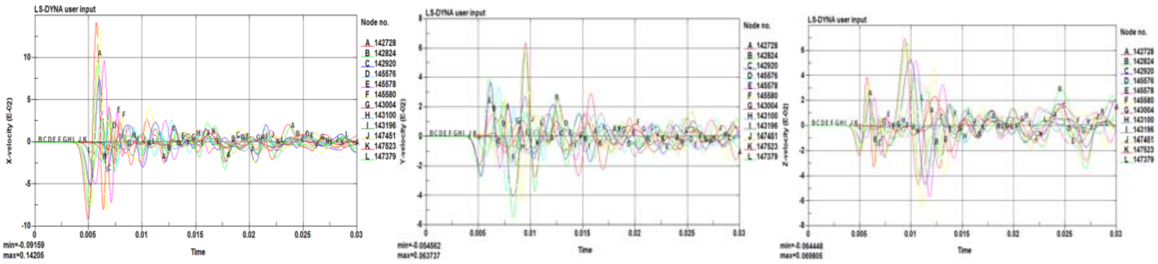

(a): X-direction *(b): Y--direction* *(c): Z--direction*

Figure 4: time history curves of velocity

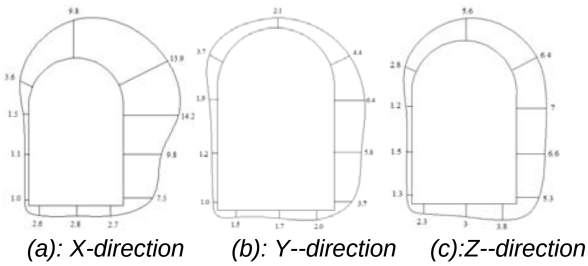

(a): X-direction *(b): Y--direction* *(c):Z--direction*

Figure 5: The envelop map of radial vibration velocity

As can be seen from the envelop map, during the process of drilling and blasting, the blast front of the existing tunnel is impacted the most, with the peak vibration velocity several to dozens of times higher than the rear one. The sequence of vibration response magnitude from top to down is the upper part of front straight wall, the middle part of front straight wall, the lower part of front straight wall, the bottom plate, and the rear straight wall. What is more, for the most prominently vibrating point, the vibration velocity along axis X is the highest, followed by the one along axis Z. The minimum speed of vibration occurs along axis Y. The tunnel front is weekly controlled during neighboring tunnel blasting excavation. It is supposed to monitor and measure the horizontal (X-direction) speed of the front. The vibration velocity of the arch spring is slightly lower than that of the upper part of the front straight wall. Nevertheless, stress is easy to concentrate on the corner of the connecting part between arch spring and the upper part of the straight wall. We allow for it and suggest that it is the section between the arch haunch and the upper part of the straight wall of the existing tunnel that should be strengthened targetedly during blasting construction, so that ensuring safe operation.
(2) The law of axial vibration velocity distribution
Figure 6 is the layout of 9 axial measurement points, and the cartridge bag lies in the grid refinement section. Each point is distributed symmetrically with the center being at the midpoint of the cartridge bag.

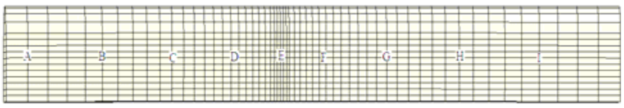

Figure 6: Layout of 9 axial measurement points

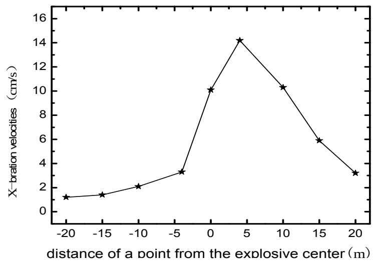

Figure 7: The envelop map of axial vibration velocity

Figure 7 shows the law of X-direction vibration velocity distribution, where points with negative distance from the explosive center are those distributed in the excavated areas behind the explosive center. As can be seen from Figure 8, the measurement points of fastest vibration fall more within the range of -4m~4m before the explosive center than the areas along the length of the cartridge bag. The reason for this phenomenon is that as the blasting excavation continues, the spacing between the pair of tunnels is narrowed constantly, rendering the distance of the explosive center from the most strongly vibrating point smaller in comparison with that from the cartridge bag.
The attenuation rate of the vibration velocity of axial measurement points in front of the explosive center is smaller than that behind the explosive center. In engineering practice, key monitoring should be done on the interval of -4m~10m from the explosive center. Meanwhile, measurement points should be placed along the straight wall as much as possible according to in-situ conditions.

3.3 Optimization simulation of the explosive loading demanded for the newly-built tunnel

To dynamically optimize the explosive loading required for tunnel blasting excavation, several numerical simulations were conducted on different sub-sections of the small-spacing tunnel. Seven typical working conditions were used to analyze the change of explosive loading, and the corresponding simulation data was shown in Table 1.

Table 1: the simulation data of typical blasting vibration

Working conditions	Tunnelface mileage (m)	spacing (m)	Explosive load (kg)	Numerical peak vibration velocity (cm/s)	Measured peak vibration velocity (cm/s)
1	DK80+354	10	72	7.0	8.4
2	DK80+360	9.7	72	9.6	11.2
3	DK80+362	8.9	48	7.8	6.6
4	DK80+366	8.2	48	10.5	9.1
5	DK80+368	8	30	6.0	6.3
6	DK80+373	7.3	30	11.9	13
7	DK80+376	6.9	24	8.2	6

The *Safety Specifications of Blasting* stipulates to use the vibration velocity as the standard for safety control, and regulates that the threshold of peak vibration velocity is 20cm/s. Pursuant to it, the monitoring value of peak vibration velocity in the engineering in this paper is set as 10cm/s, which allows for the complexity and randomness of blasting construction as well as the safety of the existing tunnel.

According to Table 1, at the spacing of 9.7m (at DK80+360), the requirement for vibration control is satisfied as the peak vibration velocity reaches up to9.6cm/s, just a little below the threshold value. The explosive loading is then reduced from 72kg to 48kg. At the spacing of 8.2m (at DK80+366), the requirement for vibration control is satisfied as the peak vibration velocity reaches up to10.5cm/s, which slightly exceeds the threshold value of 10cm/s. The explosive loading is then reduced from 48kg to 30kg. When the spacing is narrowed to 7.3m (at DK80+373), the requirement for vibration control is satisfied as the peak vibration velocity reaches up to 11.6cm/s, higher than the threshold value of 10cm/s. The explosive loading is then reduced from 30kg to 24kg.

During the tunnel blasting excavation, the explosive loading should be adjusted nonstop according to on-site monitoring conditions as the spacing continues decreasing. It is our advice to let the explosive loading be 48kg, 30kg, 24kg when the excavation is advanced to areas near DK80+360, DK80+366, and DK80+373.

4. Comparison between numerical calculation and measurement analysis

In practical engineering work, three measurement points are distributed over the front of the existing tunnel along its axis. The middle one is located in front of the tunnel face counterpart of the tunnel No.2 under construction, and moves alongside the advance of the tunnel face.

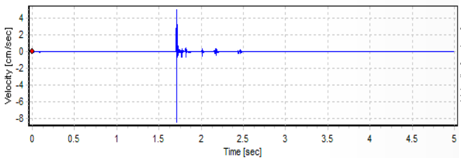

(a): Working conditions-1

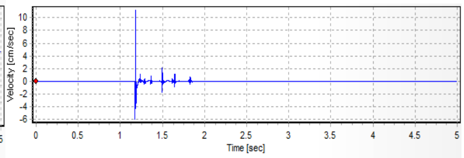

(b): Working conditions-2

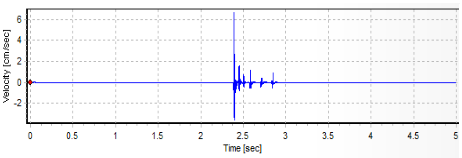

(c): Working conditions-3

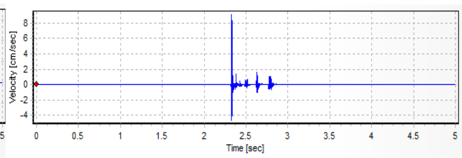

(d): Working conditions-4

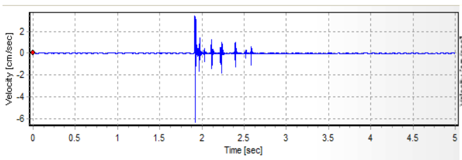

(e): Working conditions-5

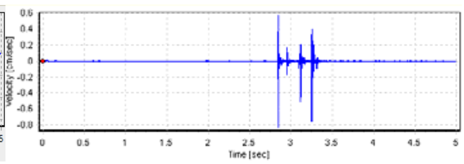

(f): Working conditions-6

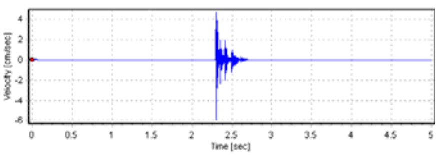

(g): Working conditions-7

Figure 8: the time history curves of measured peak vibration velocity

Vertically, the triple is located at the middle-top straight wall at intervals. Considering that the Dapiaogou tunnel and the neighboring constructed tunnel No.2 are in the same horizontal plane, such planar stress issues free us from monitoring vertical blasting vibration signals and those along the tunnel axis. Consequently, during on-site monitoring, only one radial sensor (perpendicular to the straight wall) is installed for each measurement point.

Table 1 lists the measured peak vibration velocities in different working conditions. The corresponding time history curves are plotted in Figure 8a-g. In the same working condition, the change trend of the measured result is analogous to that of the numerical result, albeit certain difference in values. Such difference can be

understandably ascribed to the existence of rock joints in comparison with the isotropic structure in our simulation.
The measured data verifies the correctness and rationality of the numerical results obtained in the paper. The dynamic response of the existing tunnel under the action of the blasting load can offset the poor predictability and hysteresis of on-site monitoring techniques. Meanwhile, the comparative result of the numerical simulation analysis and the on-site vibration test contributes to the improvement or optimization of the drilling and blasting scheme, which further helps control the blasting-induced vibration intensity.

5. Conclusion

Below are our conclusions based on the numerical simulation result in combination with the measured data:The vibration velocity at the arch spring is slightly lower than that at the upper part of the front straight wall. Nevertheless, stress is easy to concentrate on the corner of the connecting part between arch spring and the upper part of the straight wall. Therefore, the section between the arch haunch and the upper part of the straight wall of the existing tunnel should be strengthened targetedly during blasting construction.
The measurement point of fastest vibration occurs about 4m before the explosive center. In engineering practice, key monitoring should be done on the interval of -4m~10m from the explosive center.
As the spacing continues decreasing, explosive loading should be reduced reasonably. It is our advice to set the explosive loading as 48kg, 30kg, 24kg when the spacing is 9.7m, 8.2m, and 7.3m, respectively.
By comparing the numerical simulation result with the measured data, we find that the measured peak vibration velocity and the numerical results basically share the same change trend.
Proper control over explosive loading is an effective way to diminish blasting-induced vibration response and realize active management of the perniciousness of blasting-induced vibration towards the normal operation of existing tunnels. This finding is the key to offsetting poor predictability and hysteresis of on-site blasting strength monitoring methods in engineering practice.

Acknowledgments

The research is supported by the National Natural Science Foundation of China (51178388), Scientific Research Plan Project of Shaanxi Education Department (14JK1420), Central University Special Foundation for Basic Scientific Research Business of Chang’an University in China (310812161009).

References

Cafaro E., Stantero L., 2003, Fire smoke movement in tunnel scale models theory and experimental observations. International Journal of Heat and Technology, 21, 2, 161-166.
Li S., 2000, 3-D FEM Analyses on stability of Xianyueshan tunnel of Xiamen city. Chinese Journal of Rock Mechanics and Engineering, 19, 2, 211-214.
Li W., Wu Y., Fu H., Zhang J., 2015, Long-term continuous in-situ monitoring of tunnel lining surface temperature in cold region and its application. International Journal of Heat and Technology, 33, 2, 39-44. DOI: 10.18280/ijht.330205.
Liu H., 2000, Study on safety of controlled blasting of Zhaobaoshan twin tunnel with minishort separation. Engineering Blasting, 6, 1 49-55.
Tan Z., Yang X., Wng M., 2003, Effect of blast in double line tunnel on existing tunnel. Chinese Journal of Rock Mechanics and Engineering, 22, 2, 281-285.
Wang X.M., Shi W.H., Cheng Y., 2010, Effect and countermeasures of construction in new tunnel on existed tunnel. Railway Construction, 7, 80-83.
Zhao D., Wang M., 2007, Study on influence of blasting vibration on cross tunnels with small clearance. Chinese Journal of Geotechnical Engineering, 29, 1 116-119.
Zhong D., Wu L., Yu G., 2010, Effect of tunneling blasting on an existing adjacent tunnel. Explosion and Shock Waves, 30, 5, 456-462.